Journal of Infrastructure Preservation and Resilience

RESEARCH

Open Access

Effect of recycled vegetable oil on the performance of nanomarl-modified asphalt mixtures

Idorenyin Ndarake Usanga[1*], Fidelis Onyebuchi Okafor[2] and Chijioke Christopher Ikeagwuani[2]

Abstract

In response to the demand for a greener approach to pavement infrastructure and the economic benefits associated with alternative materials, the modification of neat binders has been a consistent focus. This research aimed to enhance the characteristics of asphalt binders and mixtures by incorporating recycled vegetable oil (RVO) and nanomarl. RVO was added to 60/70 penetration bitumen at concentrations of 1%, 3%, and 5% by weight, while nanomarl was kept constant at 5% by weight of the bitumen. Various physical, rheological, and microstructural properties of the modified binders were evaluated, including penetration, softening point, viscosity, rutting resistance, fatigue resistance, creep, stiffness, scanning electron microscopy (SEM), and Fourier transform infrared spectroscopy (FTIR). Furthermore, the moisture susceptibility and rutting resistance performance of asphalt mixtures incorporating these modified binders were investigated through analyses of tensile strength ratio and Hamburg wheel tracking. The test results revealed that the incorporation of RVO in bitumen led to a gradual increase in the penetration value of the modified bitumen. Simultaneously, the softening point and viscosity of the modified bitumen decreased, indicating that the addition of oil rendered the modified bitumen softer. However, the inclusion of nanomarl in RVO-modified bitumen improved its viscoelastic behavior and positively influenced its rheological properties under both unaged and aged conditions. Specifically, the addition of 5% nanomarl resulted in reduced penetration value, increased softening point, viscosity, rutting resistance, fatigue resistance, creep stiffness, and improved relaxation behavior at low temperatures. The most favorable outcomes were observed when incorporating 1% RVO with 5% nanomarl. Moreover, SEM and FTIR analysis demonstrated successful blending of the additives into the bitumen, without any evidence of phase separation. This indicates a homogeneous distribution of the additives within the bitumen matrix.

Practical application: The modification of bitumen with waste or recycled oils for the production of asphalt mixture has been successfully studied in numerous researches. However, this study introduces a novel approach by synergistically combining recycled vegetable oil (RVO) modification with the incorporation of nanomarl particles into asphalt mixture. The innovation aspect lies in the integration of two sustainable and environmentally friendly components, RVO and nanomral, to enhance asphalt performance. The findings offer a blueprint for incorporating sustainable materials and approaches in road construction projects. Pavement engineers can adopt the use of RVO modification and nanomarl particles to create longer-lasting and environmentally friendly asphalt pavements. In regions with challenging climatic conditions, the use of this modified asphalt can lead to improved infrastructure resilience. Roads built with these materials can better withstand temperature fluctuations. The integration of RVO and nanomarl particles

*Correspondence:
Idorenyin Ndarake Usanga
idorenyinusanga@aksu.edu.ng
Full list of author information is available at the end of the article

offers improved performance, cost-effectiveness, reduced environmental impact, and also opens avenue for further exploration and optimization of asphalt mixtures incorporating innovative additives.

Keywords Nanomarl, Recycled Vegetable Oil, Viscosity, Rutting Resistance, Fatigue Resistance, Creep Stiffness

Introduction

The growth of urban population worldwide has resulted in an increased demand for infrastructural development. This has prompted the government of most nations to commit huge amount of financial resources to the expansion of existing facilities and the construction of new pavements with its attendant financial strain on the lean resources of nations. In fact, annual global production of asphalt mixes for pavement construction is estimated to exceed one billion ton per year [1]. Consequently, there has been a significant demand for bitumen, a key component in asphalt pavement. The use of bitumen, a non-renewable petroleum material, is associated with factors that often do not conform to green revolution in pavement infrastructures such as carbonization, environmental pollution and fossil energy consumption. Given the aforementioned concerns, researchers and pavement engineers are now considering the utilization of alternative bitumen material thatare sustainable, environmentally friendly, energy efficient [2] and ultimately conform to green pavement design. One of such alternative materials is bio-mass source. And a typical example of bio-mass source is recycled vegetable oil (RVO) used to amend or substitute bitumen in the production of asphalt mixes.

The utilization of different types of waste or recycled oils in asphalt pavement has become increasingly popular due to its numerous reported advantages which include availability, cost-effectiveness, and improved performance offered by them in terms of enhanced low temperature resistance and workability [3]. Remarkably, the rise in population growth has resulted in an increased demand for food, leading to the generation of large amounts of kitchen wastes. One of the most common forms of kitchen wastes is used vegetable oil, which is a waste material produced from the frying of foods with pure vegetable oil in most households, hotels, restaurants, and catering establishments. Improper disposal of this waste oil causes unwarranted environmental pollution, increases water channel blockages, and contaminates both land and water habitats. Moreover, the consumption of this waste oil sometimes have detrimental effects on human and animal health. Interestingly, there has been a growing commitment towards the utilization of sustainable pavement materials and also to mitigate the disposal challenges of used vegetable oil. This commitment has led to the recycling of used vegetable oil in order to minimize its detrimental effects.

When vegetable oil is used for frying of foods, the high temperatures, which typically ranges from 160 to 200 °C, induces dissociation of its hydrocarbon chains from the glycerol backbone in the fatty acids leading to the liberation of glycerol molecules. The residual fatty acid chains subsequently undergo a series of chemical transformations, including oxidation and polymerization. These reactions result in the formation of intricate hydrocarbon structures, specifically triglycerides, which consists of three fatty acid chains bonded to a glycerol molecule [4]. From a chemical perspective, bitumen is characterized as a viscous and viscoelastic liquid composed mainly of hydrocarbons and their derivatives. It is soluble in toluene, exhibits low volatility, and exhibits gradual softening upon heating [5]. Bitumen can be categorized into two main constituents: asphaltene and maltenes. The interaction between asphaltenes and recycled vegetable oil can lead to the dispersion and stabilization of asphaltenes within the oil phase. This can result in the modification of the rheological properties and stability of the bitumen-oil mixture. On the other hand, maltenes can contribute to the overall solubility and compatibility of bitumen with recycled vegetable oil, facilitating the blending and homogenization of the two materials.

In the last decade, many studies have been implemented on the use of recycled waste cooking oil to improve the performance of binder in asphalt mixtures. In a study conducted by Bilema et al. [6] the rheology and physical properties of asphalt binder blended with waste cooking oil were investigated. The findings revealed that the addition of waste cooking oil had the potential to soften the asphalt binder, resulting in a softer asphalt binder. However, it was observed that the use of waste cooking oil in the blend led to a reduction in the rutting resistance of the asphalt mixture. Similarly, Ahmad et al. [7] conducted a study on aged asphalt with an oil extracted from discarded fruit. The study revealed improvements in workability and coating of the asphalt mixture. Furthermore, Guarin et al. [8] utilized fish oil to restore the properties of reclaimed asphalt pavement binder. Previous research has also indicated that waste cooking oil (WCO) can enhance certain physical characteristics of aged asphalt, including penetration and softening point. Wen et al. [9] investigated the performance

of WCO as an alternative binder under high and low temperatures. The rheological analysis demonstrated a reduction in the complex modulus (G*), leading to a decrease in rutting resistance at high temperatures. From the aforementioned literature, it can be concluded that waste oils provide benefits to the low temperature performance of asphalt binders. However, they do not have the capability to enhance the high temperature performance of binders.

When waste cooking oil is incorporated into bitumen for asphalt production, it presents certain challenges, particularly regarding the high-temperature performance of the binder. Waste oil, especially used cooking oil, contains volatile components, including triglycerides and fatty acids such as lauric acid, palmitic acid, oleic acid, and linoleic acid. These volatile components undergo vaporization and thermal decomposition, resulting in a reduction in the effective binder content [10]. As a consequence, the blended mixture becomes softer and more susceptible to rutting and deformation at high temperatures. To address this challenge, a range of additives is often used to improve the high-temperature resistance of the binder in bitumen-waste oil blends. These additives includes polymers, anti-stripping agents, antioxidants, and rejuvenators, among others [11]. Admittedly, extensive studies have provided compelling evidence that the incorporation of these additives into the blend leads to an improvement in the high-temperature performance of the binder, effectively addressing concerns such as softening, rutting, and deformation at elevated temperatures [12–16]. Nonetheless, it is important to acknowledge that the utilization of many of these additives is accompanied by certain limitations. In fact, they are often criticized for their high cost, poor storage stability, environmental concerns, and potential for bleeding [17]. In order to overcome these limitations, it is advantageous to consider the utilization of an additive such as nano clay, which has the potential to address these concerns effectively. The utilization of nanomaterials, particularly nanoclays due to their high surface area, has become increasingly popular in the field of pavement engineering [18, 19]. Nanoclays are small particles composed of layered mineral silicates. They belong to various classes such as halloysite, kaolinite, hectorite, bentonite, and montmorillonite depending on nanoparticle structure and their chemical composition.

A plethora of studies have been conducted on the application of nanoclay for the modification of asphalt binder. Jahromi et al. [20] conducted a study to assess the impact of two types of nanoclay such as Nanofill-15 and Closite15A on asphalt binder and mixtures. Their findings revealed that the addition of nanoclay led to increased stiffness, indirect tensile strength, resilient modulus, and Marshall stability, thereby improving rutting resistance. In another study conducted by Goh et al. [21], nanoclay and carbon microfiber were incorporated into the binder, and the resulting mixtures were evaluated for tensile strength and moisture susceptibility. The test results demonstrated that the inclusion of nanoclay enhanced the mechanical properties of the asphalt mixtures. Specifically, specimens containing 1.5% nanoclay exhibited higher tensile strength, and the moisture susceptibility performance was also improved. Similarly, Nazzal et al. [22] examined the performance of bitumen modified with Cloisite 20A composite nanoclay. Two modification percentages, 2% and 4% by weight, were investigated. The study revealed that nanoclay enhanced the stiffness and hardness of the asphalt binder at various temperatures.

It is fascinating to note that there are abundant reserves of clay in different regions worldwide, yet many of them remain largely unexplored and underutilized. One such example is Marl, which is found in various locations[23]. Marl is a specific type of mudstone characterized by its composition of clay and varying amounts of calcium carbonate, typically ranging between 35 and 65% [24]. Despite its potential, Marl has not received significant attention in many areas where it is found. It is important to highlight that heat-treated marl has been used as a filler in asphalt mixtures, as a supplementary cementitious material in concrete, and in various civil engineering applications involving geopolymer materials [25–27]. Despite the lack of extensive exploration, the potential of utilizing nano marl as an additive to enhance the high-temperature performance of bitumen-recycled oil blend binders in asphalt mixtures has been largely unexplored. Therefore, this study aims to fill this research gap by evaluating the physical and rheological properties of a recycled vegetable oil-bitumen blend, incorporating the nano marl additive.

Materials and methods

Material

Binder

The 60/70 penetration grade bitumen used in this study was obtained from Basse Engineering services, Nigeria. This particular grade of bitumen is extensively utilized in various bituminous mixtures in Nigeria because of its versatility and adaptability to a wide temperature range. The essential physical properties of this binder for three (3) samples each are presented in Table 1.

Aggregate

The study utilized crushed aggregates, including coarse and filler materials, which were sourced from a quarry located in Netim, Cross River State. The coarse

Table 1 Physical properties of bitumen

Test	Standard Adopted	Value	Standard Requirement	Standard Error
Penetration at 25 °C (0.1 mm)	ASTM D5 [28]	67	60–70	1.0
Softening point (^{o}C)	ASTM D36 [29]	48.5	min 46	0.3
Brookfield rotational viscosity at 135^{0}C (MPa.s)	ASTM D4402 [30]	560	< 3000 mPa.s	10
Flash Point (^{o}C)	ASTM D92 [31]	250	min 230	2
Specific gravity (g/cm^{3}) Penetration index (PI)	ASTM-D70 [32]	1.02 -1.95	1.01 – 1.06 -	0.02 0.03

Table 2 Physical properties of aggregates

Test	Standard Adopted	Value	Standard Requirement	Standard Error
Coarse				
Angularity (%)	ASTM D5821 [33]	98/97	≥55%	1.5
Elongated and flat particles (%)	ASTM D4791 [34]	6.94	< 20%	1.7
Soundness (%)	ASTM C88 [35]	0.069	< 20%	0.5
Specific gravity	ASTM C127 [36]	2.564	2.6 – 2.9	0.01
Los Angles abrasion (%)	ASTM C131 [37]	23.7	< 30%	2.2
Water absorption (%)	ASTM C127 [36]	1.98	≤2%	0.9
Fine				
Absorption	ASTM C131 [37]	1.77	≤2%	0.01
Specific gravity	ASTM C128 [38]	2.60	2.5 – 2.8	0.02
Sand equivalent	ASTM D2419 [39]	77.01	≥50%	1.8
Clay content (%)	ASTM C142 [40]	0.61	< 5%	0.06
Filler				
Specific gravity (g/cm^{3})	ASTM C854 [41]	2.58	-	0.01
Specific Surface area (m^{2}/kg)	ASTM C204 [42]	420	-	3
Percentage passing sieve no. 200	ASTM D546 [43]	92	75—100	1.5

aggregates were of granite origin while the mineral filler was of limestone aggregate source. Furthermore, the fine sand used in the study was obtained from a natural deposit in Ibesikpo Asutan, Akwa Ibom State. The physical properties of these aggregates for three (3) samples each, based on ASTM international materials grading standards, are provided in Table 2.

Additives

Nanomarl Nanomarl was manufactured from marlstone sourced from a natural deposit in New Netim, Cross River State, Nigeria. Upon collection, it underwent a drying process in an oven at 100 °C for 5 h to eliminate moisture content. Thereafter, the marlstone was ground into tiny particles to achieve a micro-size. These particles were subsequently transformed into nano-size through a gradual heating process up to 650 °C using an electric furnace. The nanomarl samples were examined for particle size distribution using Transmission Electron Microscopy to analyze their structure, while X-ray Fluorescence was employed to determine the chemical composition. The detailed characterization results of the nanomarl can be found in Tables 3 and 4.

Table 3 Particle size distribution of nanomarl

Property	Nanomarl	Standard Error
Particle size range	5 – 8 nm	0.03
Average crystalline size	5 nm	0.01
Particle distribution	Well distributed	-

Recycled vegetable oil The recycled vegetable oil (RVO) employed in this research was sourced from a restaurant, where it was collected and subjected to filtration to eliminate any dirt or impurities. The basic physical and chemical compositions of the RVO are presented in Tables 5 and 6, respectively.

Table 4 Chemical composition of nanomarl

Chemical Composition	Content (%)
Silicon oxide (SiO_2)	49.60
Aluminum oxide (Al_2O_3)	13.234
Iron oxide (Fe_2O_3)	8.391
Calcium oxide (CaO)	14.21
Magnesium oxide (MgO)	1.599
Potassium (K_2O)	3.266
Sodium (Na_2O)	0.167
Titanium oxide (TiO_2)	0.881
Sulfur trioxide (SO_3)	2.354

Table 5 Basic physical properties of RVO

Test	Value	Standard Error
Density (g/cc)	0.92	0.01
Viscosity (mPa.s) 40^0C	73	5
Flash point ^{o}C	265	8

Table 6 Chemical composition of RVO

Chemical	Content
Triglyceride	78.9
Diglyceride	1.76
Monoglyceride	2.2
Free fatty acid	1.63
pH	5.36

Methods

Preparation of bitumen-RVO-nanomarl blend by wet process

First, the base binder was heated and continuously stirred in a pressure container until it reached a temperature of 135 °C. Subsequently, the recycled vegetable oil (RVO) was added to the bitumen at different concentrations of 1%, 3%, and 5% by weight of the bitumen. The mixture was stirred using a high shear mixer at 3800 rpm for a duration of 20 min. Following this, the nanomarl, which accounted for 5% by weight of the bitumen, was gradually introduced to the bitumen-RVO blend. The constant nanomarl content of 5% was based on preliminarily investigation involving different nanomarl percentages. The preliminarily test indicated that 5% nanomarl consistently demonstrated significant improvement in asphalt mixtures [44]. The entire mixture was then heated to a temperature of 165 °C and stirred at 5000 rpm for 40 min to ensure the formation of a homogeneous blend. A total of 4 specimens with different compositions designated as NB (neat binder), NB15 (neat binder + 1% RVO + 5% nanomarl), NB35 (neat binder + 3% RVO + 5% nanomarl), NB55 (neat binder + 5% RVO + 5% nanomarl) were obtained from the mixture of bitumen, recycled vegetable oil and nanomarl. In all the tests conducted, three replicate samples were prepared and analyzed. This approach of replicating the samples ensures the reliability and accuracy of the results by reducing the potential for random variations or errors.

Mixture design and preparation

To evaluate the performance of this modified binders in asphalt mixtures, dense graded mixture with maximum aggregate size of 19 mm as shown in Fig. 1 was used.

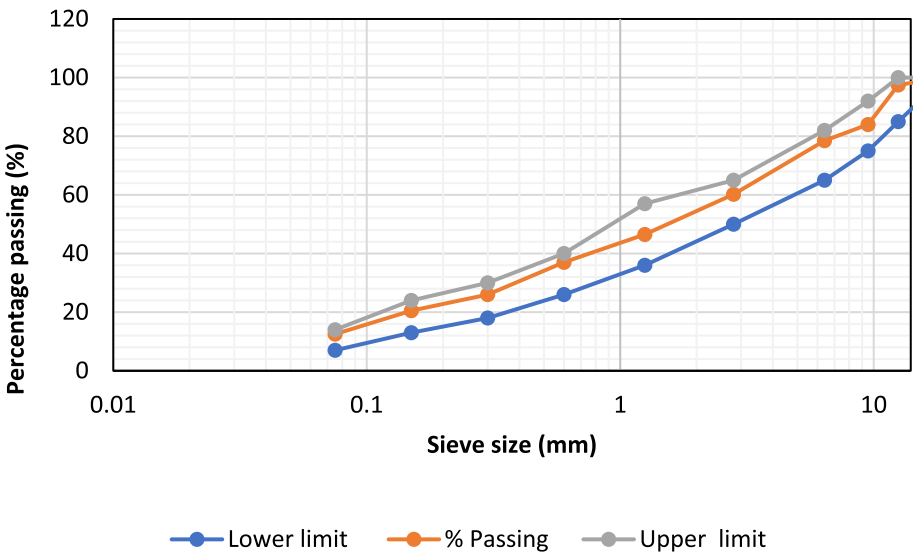

Fig. 1 Asphalt mixture gradation curve

Initially, a gradual increase in the bitumen content (BC) ratio, ranging from 4.5% to 6.5%, was used to determine the optimum bitumen content (OBC), which was then used for preparing the modified set of samples. The modified set comprised three different compositions, namely NB15, NB35, and NB55, as previously mentioned. These compositions were added based on the weight of the OBC which was estimated to be 5%. The determination of the OBC followed the procedures outlined in ASTMD1559 [45] which specifies the methods for conducting the Marshall stability and flow tests used in OBC determination. The preparation of the modified asphalt mixtures involved heating the aggregates to a temperature of 175 °C until they were completely dry. Simultaneously, the binders were heated to a temperature of 155 °C. The necessary amount of heated binder was then introduced to the heated aggregates, and the mixture was thoroughly blended at a temperature of 160 °C using a mechanical mixer, following the guidelines outlined in ASTMD1559 [45]. Figure 2 illustrates the experimental procedure for the preparation and testing of binders and asphalt mixtures.

Binder performance test

Physical properties Three physical tests were carried out on both the neat binder and the modified binders. These tests included the penetration test, softening point test, and rotational viscosity test. The penetration test followed the ASTM D5 [28] standard, while the softening point and rotational viscosity tests were conducted in accordance with the ASTM D36 [29] and ASTM D4402 [30] standards, respectively. Each physical test was performed three times for all the specimens. The rotational viscosity test employed the Brookfield rotational viscometer, while the softening point test utilized the ring and ball apparatus.

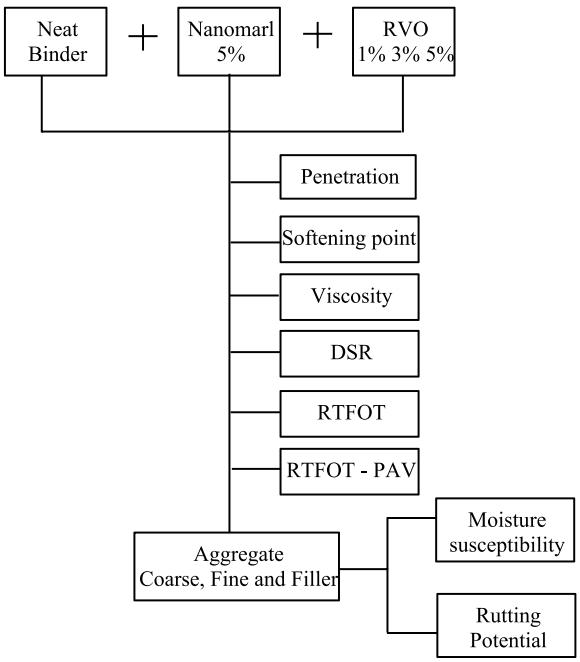

Fig. 2 Schematics of experimental procedure for the preparation and testing of binders and asphalt mixtures

Rheological properties

i) Unaged binders

The rheology of the unaged binders were conducted using a dynamic shear rheometer (DSR). Following the guidelines of AASHTO T 315 [46], the tests were performed at various temperatures to replicate the conditions of the test location, including 35 °C, 46 °C, 58 °C, and 65 °C. To initiate the test, the upper and lower plates of the DSR were heated to the desired test temperature to ensure proper adherence of the specimens. Subsequently, the specimens were positioned between the upper and lower plates and allowed to come together to achieve the desired testing gap and the testing frequency maintained at 10 rad/s, as specified in the test standard. Afterward, the DSR software was utilized to calculate the maximum applied stress (σ) and the corresponding maximum strain (τ). The complex shear modulus (G*) was then determined using Eq. (1). The phase angle (δ) was determined by analyzing the time lag between the occurrence of σ_max and τ_max.

$$G^* = \frac{\sigma_{max}}{\tau_{max}} \tag{1}$$

where, σ_{max} is the maximum stress; τ_{max} is the maximum strain.

To assess the potential for rutting in a binder, the rutting factor, represented as G*/Sin(δ), is determined. The rutting factor serves as a measure of the binder's ability to resist permanent deformation. A higher rutting factor indicates better elasticity and resistance to rutting. However, it should be noted that for an unaged binder, the minimum acceptable value for G*/Sin(δ) is specified as 1.0 kPa [46]. This requirement ensures a certain level of performance and resistance to rutting in the binder.

ii) Aged binders

The binders were subjected to aging processes, both in the short-term and long-term. Short-term aging refers to the changes that occur in the asphalt binder shortly after

production and exposure to environmental and operational conditions. These changes are caused by factors like oxidation, volatilization of lighter components, and molecular rearrangement. Short-term aging can result in increased viscosity, stiffening of the binder, and diminished workability and adhesive properties. These changes can impact the performance of asphalt mixtures, affecting their workability during construction and the durability of the pavement. The short-term aging of the binder was assessed using the Rolling Thin Film Oven Test (RTFOT) following the prescribed procedures outlined in AASHTO T-240 [47]. The test involved subjecting the binder to a temperature of 163°C in the RTFO bottle for a duration of 85 min. In contrast, long-term aging corresponds to the gradual deterioration of the asphalt binder throughout its service life. Factors like exposure to sunlight, temperature variations, moisture, and traffic loading contribute to this long-term aging process. As time passes, the binder tends to undergo hardening, brittleness, and a decline in desirable properties. These changes result in reduced flexibility, increased susceptibility to cracking, and a decrease in resistance to deformation under traffic loads. To assess the long-term aging of the binder, the residues obtained from the RTFO test were employed in the Pressure Aging Vessel (PAV) apparatus. The PAV test, lasting 20 h, aimed to simulate the effects of extended aging on the binder.

iii) Aged binders at low temperatures

The long-term aged binders were tested for their performance at low temperatures and susceptibility to thermal cracking using the Bending Beam Rheometer (BBR). The BBR test was conducted using an Applied Test Systems apparatus, following the guidelines outlined in AASHTO T313 [48]. Three different temperatures were selected for the test: 0 °C, -6 °C, and -12 °C. The test procedures involve immersing bitumen beams with dimensions of 127 mm in length, 6.4 mm in thickness, and 12.7 mm in width into a temperature-controlled bath for a duration of 60 min. After preloading, a constant load of approximately 100 g is applied to the rectangular beam, which is supported on stainless steel half rounds at both ends. The deflection from the center of the beam is continuously measured, and the creep rate (m) and stiffness of creep (S) are determined at various loading times ranging from 8 to 240 s. The BBR test provided an evaluation of the long-term aged binder's behavior at low temperatures, offering insights into its ability to withstand thermal cracking under different temperature conditions. The measurements of creep rate and stiffness of creep offered valuable information about the binder's stiffness and deformation characteristics at low temperatures.

Asphalt mixtures performance test

Moisture susceptibility The moisture susceptibility of asphalt mixtures with these modified binders were evaluated using the modified Lottman test. This test involves comparing the indirect tensile strength results of a dry sample and a sample immersed in water. The test procedure followed the guidelines outlined in AASHTO T 283 [49] guidelines. For each mixture, six specimens were tested to determine both the indirect tensile strength and the tensile strength ratio. The mixture specimens were divided into two sets. The first set, consisting of three specimens, was evaluated without moisture conditioning after being compacted to an air void of 8%. The second set was also compacted to the same air void but underwent conditioning by soaking in water heated to 65 °C before being tested at 25 °C. The specimens were then subjected to the indirect tensile strength test. During the test, a compressive force was applied steadily along the diametrical plane of the samples at a rate of 50.8 mm/min until failure occurred. Equation (2) was utilized to calculate the indirect tensile strength, while Eq. (3) was employed to determine the tensile strength ratio.

$$ITS = \frac{2P}{\pi t_s d_s} \tag{2}$$

where, ITS corresponds to the indirect tensile strength (expressed in Pa).; P is the maximum applied load on specimen (measured in N); t_s is the thickness of specimen (measured in mm); and d_s denotes the diameter of specimen (measured in mm)

$$TSR = \frac{ITS_w}{ITS_d} \tag{3}$$

where, TSR represents the tensile strength ratio; ITS_w denotes the indirect tensile strength at wet condition; and ITS_d represents the tensile strength at dry condition.

Rutting potential To evaluate the potential for rutting in these binders, the Hamburg wheel tracking test (HWTT) was employed. The HWTT is a well-known laboratory simulation test designed to assess the resistance to rutting and moisture susceptibility in hot mix asphalt. Following the guidelines outlined in AASHTO T 324 [50], the HWTT was conducted in this study. For each mixture, two cylindrical specimens with dimensions of 150 mm in diameter and 62 mm in height were prepared. These specimens were immersed in a hot water bath maintained at a temperature of 50 °C. Steel wheels, measuring 203 mm in diameter and 47 mm in width, were brought into contact with the cylindrical specimens and subjected to 52 passes per minute. Throughout the

test, the vertical displacements of each wheel were continuously monitored using a linear variable transducer (LVT). The rutting depths of the specimens were measured as the test progressed. The test was terminated when the maximum rutting depth reached either 10 mm or after 20,000 load passes, whichever occurred first. This criterion determined the point at which the test was considered to have reached failure.

Microstructural evaluation of binders

The rheological properties of asphalt mixtures are influenced by alterations in surface topography, molecular groups, and dispersion characteristics of modified bitumen. These modifications can lead to changes in the flow behavior, viscosity, and overall performance of the asphalt mixtures**.** Fourier transform infrared spectroscopy (FTIR) analysis was conducted to identify and characterize the functional groups present in both the bitumen and the bitumen blend. The purpose of this analysis was to determine the specific chemical bonds and functional groups within the samples and gain insights into their composition and structure [51]. In this study, the FTIR was performed using Agilent technologies, which utilizes a transmittance method within a wavelength range of 650 to 4000 cm^{-1} and a resolution of 8 cm^{-1}. Also, the dispersion characteristics and homogeneity of binders were investigated using scanning electron microscopy (SEM). The SEM analysis was performed using the Phenom World electron microscope. Prior to analysis, the specimens were coated with a thin layer of gold, approximately 1.5 to 3 mm in thickness, using sputter coater equipment. The purpose of this coating was to prevent poor image quality and electrostatic charging during the testing process.

Cost analysis

A comprehensive cost analysis was conducted to compare the production costs of one metric ton of both modified and unmodified asphalt mixtures. This evaluation centered on the optimal modified mixture, specifically NB15 (consisting of 1% RVO and 5% nanomarl). The analysis focused solely on the direct material costs entailed in the mixtures, encompassing coarse aggregate, fine aggregate, mineral filler, bitumen, as well as the employed modifiers (RVO and nanomarl). Of particular note, the material cost of RVO was treated as negligible in this assessment due to its status as a waste material. However, it is worth mentioning that the cost of transporting this waste material within a 2 km radius was factored into the estimate, amounting to N3000 per ton. Notably, the analysis excluded indirect production costs and profits from consideration, as they were presumed to remain relatively constant across all mixtures. This approach allows for a focused examination of the direct material expenses, shedding light on the comparative cost dynamics between the modified and unmodified asphalt mixtures.

Results and discussions

Physical properties of binders

Penetration

The penetration value of a binder serves as an indicator of its homogeneity, providing insights into its rheological properties [52]. This empirical relationship helps to assess the consistency and uniformity of the binder. The results of the penetration test for the binders are depicted in Fig. 3. As observed in Fig. 3, the incorporation of additives led to a decrease in the penetration values. However, increasing the content of RVO resulted in higher penetration values for the modified binders. Typically, the addition of RVO to neat bitumen is expected to render the binder softer. However, the inclusion of 5% nanomarl particles introduced a hardening effect due to their large surface area and unique surface chemistry, which can adsorb onto the bitumen's molecules. This adsorption modifies the molecular structure of the bitumen, leading to an increase in its viscosity, counteracting the anticipated softening effect of RVO [53].

Softening point

The softening point of a binder indicates its capacity for plastic flow and serves as an indicator of its stability at high temperatures [54]. Generally, a higher softening point implies enhanced stability of the binder when subjected to elevated temperatures. The softening point values of both the neat and modified binders are illustrated in Fig. 4. As depicted in Fig. 4, the addition of a blend comprising waste cooking oil (RVO) and nanomarl resulted in an increase in the softening point of the neat binder, except at higher RVO contents where no significant difference was observed compared to the neat binder. Specifically, the modified binders NB15 and NB35 exhibited softening point increases of 24% and 15.7%, respectively, while the improvement in softening point for NB55 was only 0.6%, which is considered insignificant. This phenomenon can be attributed to the interplay of interactions introduced by nanomarl particles. These interactions encompass enhanced molecular binding, viscosity augmentation, structural stabilization, and the potential for complexation and crosslinking with RVO. The combined effects of these diverse chemical processes

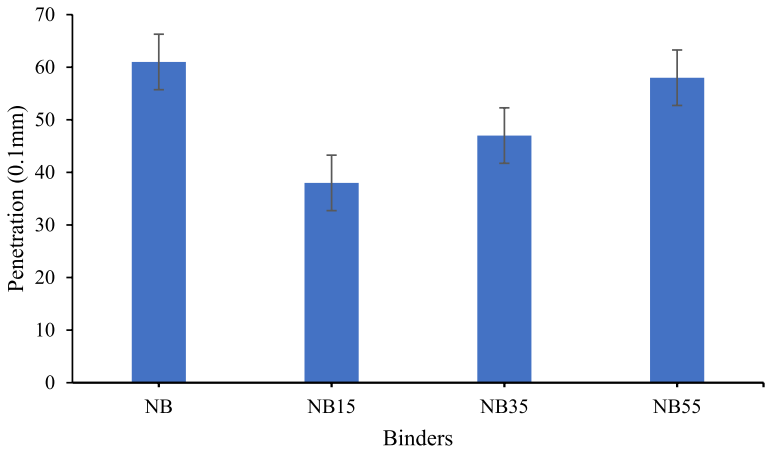

Fig. 3 Penetration values of binders

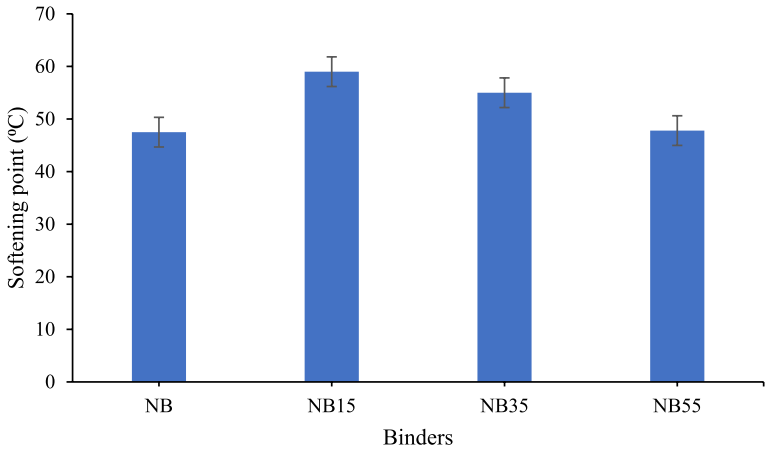

Fig. 4 Softening point of binders

culminate in an increased softening point, signifying an increased resistance to temperature-induced softening and deformation [55].

Rotational viscosity

Viscosity serves as an indicator of the stiffening effect in the bitumen-RVO-nanomarl composite binder. The rotational viscometer test was conducted at a temperature of 135°C for all samples, and the results are presented in Fig. 5. It was observed that the addition of 1% and 3% RVO with constant 5% nanomarl significantly increased the viscosity of the binder. However, the inclusion of 5% RVO slightly reduced the viscosity. The viscosity of NB55 was determined to be 0.47 Pa.s, while the viscosity of the neat binder (NB) was 0.48 Pa.s. Overall, the viscosities of the binders remained within the acceptable limit specified as 3 Pa.s at 135°C according to the SHRP specification.

Rheological properties

Rutting resistance

The results regarding the rutting resistance of the unaged and short-term aged binder are displayed in Figs. 6 and 7. The rutting resistance, represented by the parameter $G^*/Sin(\delta)$, primarily reflects the stiffness properties of the binder. As observed in Fig. 6, the incorporation of the composite additive, specifically up to 3% RVO and 5% nanomarl, improved the rutting resistance of the neat binder. The peak improvement was observed at 1% RVO with 5% nanomarl, demonstrating an 18.2% increase in rutting resistance compared to the neat binder. However, at 5% RVO, there was no significant enhancement in the rutting resistance of the binder. This improvement in the binder's performance at high temperatures can be attributed to the presence of CaO in the marl, as identified by its chemical composition in the XRF analysis. CaO acts as

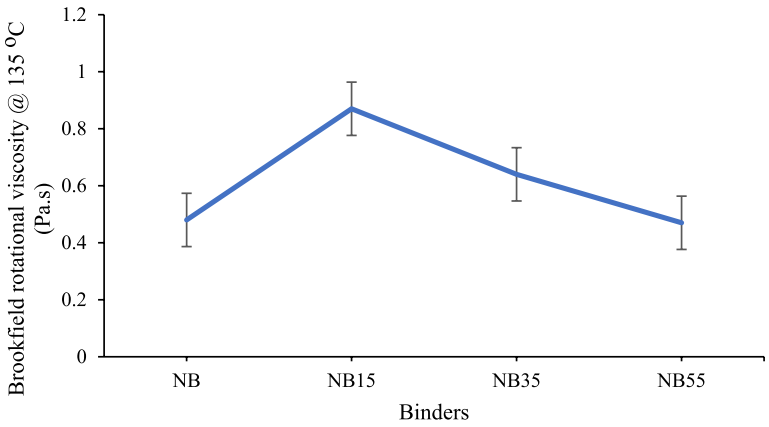

Fig. 5 Rotational viscosity of binders

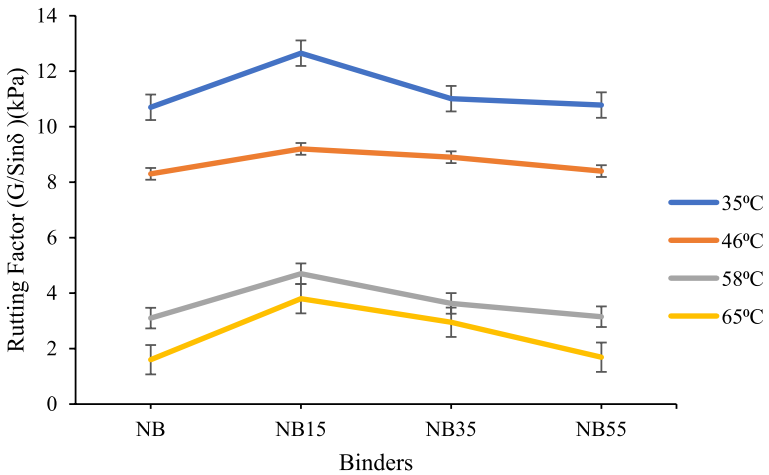

Fig. 6 Rutting resistance of unaged binders

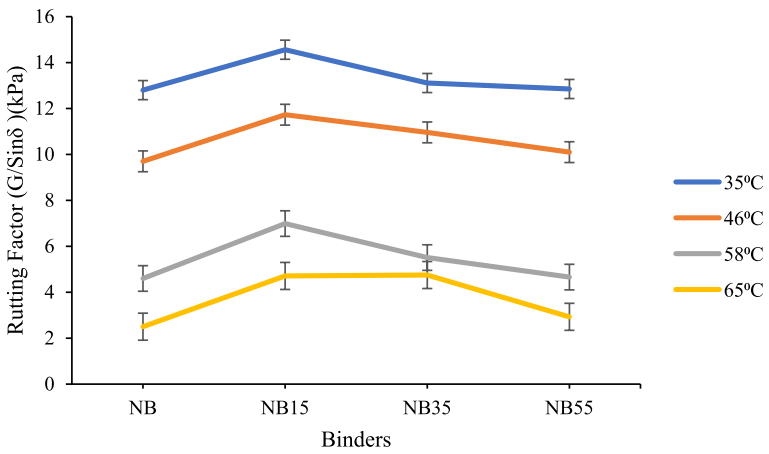

Fig. 7 Rutting resistance of short-term aged binders

an anti-rutting additive [27], create bonds that enhance the cohesion and adhesion of the binder. This cohesion prevents the binder from shearing or flowing excessively, which is crucial for resisting rut formation. Furthermore, the rutting resistance of the binders under RTFOT- short-term aged conditions is illustrated in Fig. 7. Similar to the findings in the unaged condition, the binder aged through RTFOT with 1% RVO and 5% nanomarl exhibited a higher value of G*/Sin(δ) compared to the neat binder. This indicates that the inclusion of the specified content of composite additives enables the binder to withstand higher temperatures and oxidation rates resulting from production and exposure to environmental and operational conditions. The enhanced rutting resistance observed in the aged binder further supports the effectiveness of the composite additives in improving the short-term performance of the binder.

Fatigue resistance

Figure 8 presents the impact of varying percentages of RVO, while maintaining a constant nanomarl content, on the fatigue resistance of the binder. The inclusion of nanomarl, combined with the specified content of RVO, enhances the stiffness and strength of the binder matrix, resulting in a reduction in fatigue crack propagation within the binder. However, when the RVO content reaches 5%, the improvement in fatigue crack resistance is not as significant compared to the neat binder. Specifically, at 19°C, the fatigue resistance shows an improvement of 18.1% and 5.89% for RVO contents of 1% and 3%, respectively, whereas the improvement is only 0.25% for a 5% RVO content. This observation can be attributed to the presence of a good interfacial bonding between the bitumen and nanomarl, as indicated by the SEM results. The enhanced interfacial bonding contributes to the improved fatigue resistance of the binder.

Creep rate and stiffness

Figures 9 and 10 showcase the stiffness (S) and creep rate (m) of the binder after aging using the RTFO and PAV methods. These parameters provide valuable insights into the fracture resistance and stress relaxation characteristics of the binder, particularly at low temperatures. A low creep stiffness value indicates a binder with improved resistance to cracking at low temperatures and fewer fractures. The phenomenon behind this performance can be attributed to the fact that at low temperatures, the modified bitumen with RVO and nanomarl particles maintains a more fluid-like behavior compared to conventional bitumen. This is due to the combination of plasticization effects from RVO and the dispersing effect of nanomarl particles. The lower viscosity at low temperatures minimizes the tendency for crack initiation and propagation, reducing the brittleness that can lead to failure. Conversely, a high creep rate suggests that the binder exhibits a lower level of stress relaxation performance. According to the guidelines outlined in AASHTO M320 [56], the desired criteria are a creep stiffness (S) value below 300 mPa and a creep rate (m) value above 0.3.

Figure 9 demonstrates that the introduction of nanomarl into the bitumen has an impact on the creep stiffness of the binder. The inclusion of 5% nanomarl into the bitumen-RVO blend contributes to increased stiffness within the binder matrix, resulting in higher creep stiffness values, particularly at low temperatures. Nanomarl particles have a high aspect ratio and a large surface area, which allows them to form a network-like structure within the bitumen matrix. This

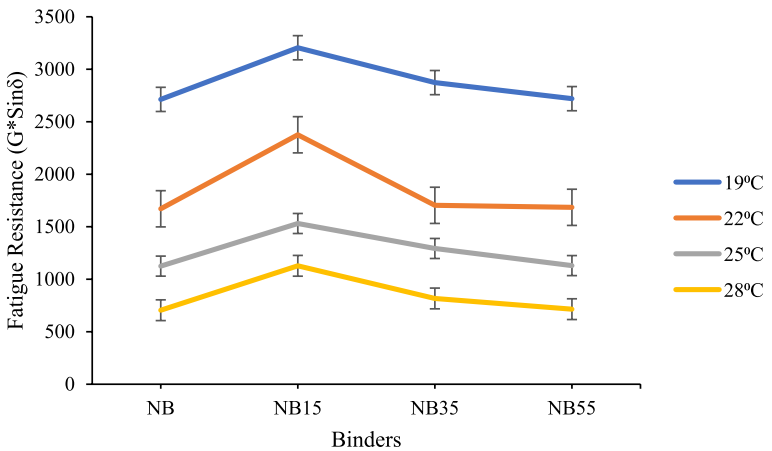

Fig. 8 Fatigue resistance of RTFOT-PAV long term aged binders

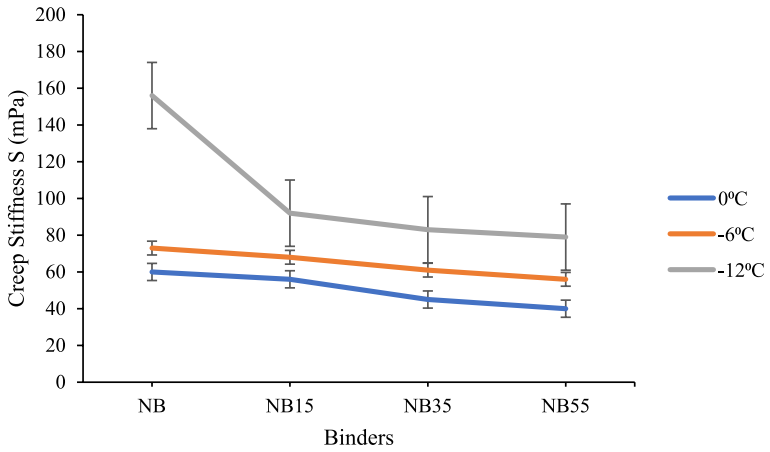

Fig. 9 Fracture resistance of binders at low temperatures

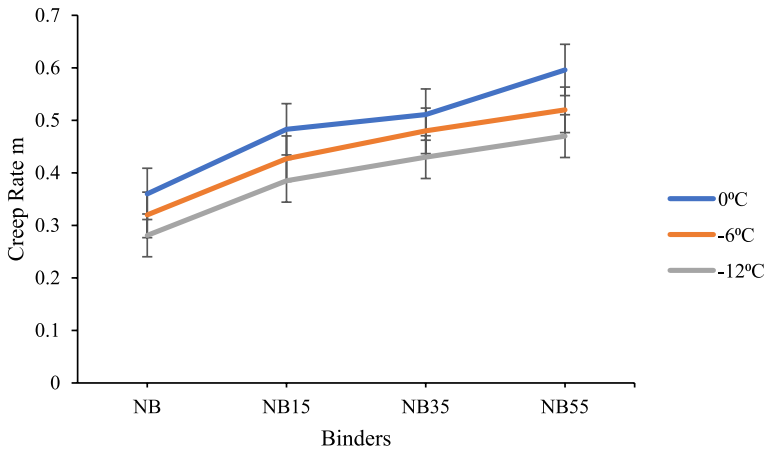

Fig. 10 Stress relaxation of binders at low temperatures

reinforcement effect enhances the stiffness and modulus of the binder, making it more resistant to deformation and creep under applied loads. On the other hand, Fig. 10, which represents the creep rate, shows an inverse relationship to the creep stiffness. This suggests that the addition of RVO in moderate amounts can improve the relaxation behavior of the binder at low temperatures. A higher creep rate indicates a greater ability of the binder to relax stress, which is beneficial in reducing the risk of cracking under cyclic loading conditions. Overall, these findings indicate that the incorporation of these additives can influence the creep stiffness and creep rate of the binder, potentially enhancing fracture resistance and stress relaxation performance at low temperatures.

Asphalt mixtures performance

Moisture susceptibility

To assess the moisture susceptibility of asphalt mixtures incorporating these binders, two key sets of results are necessary: the indirect tensile strength of conditioned and unconditioned specimens, and the tensile strength ratio. Figure 11 presents the outcomes for the indirect tensile strength of unconditioned (25°C) and conditioned (65°C) mixtures. It is evident from Fig. 11 that the indirect tensile strength slightly increases with the addition of 1% and 3% RVO with 5% nanomarl, followed by a decrease to nearly the same value as the neat binder. The tensile strength ratio (TSR), representing the ratio of conditioned to unconditioned asphalt specimens for each binder, is depicted in Fig. 12. It can be

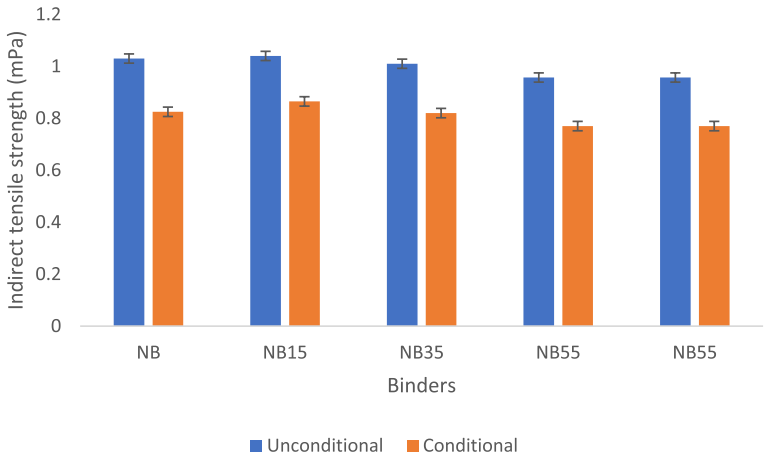

Fig. 11 Indirect tensile strength for conditioned and unconditioned of asphalt mixtures

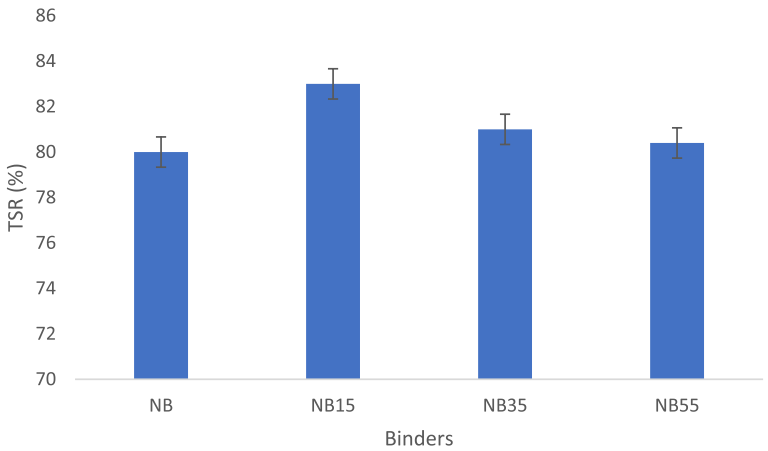

Fig. 12 Tensile strength ratio for asphalt mixtures

observed that both the neat binder and modified binders meet the specifications outlined in AASHTO T-283 [49], which establishes a minimum value of 80% TSR. The good performance of the unmodified binder can be attributed to the effect of limestone mineral filler used in the study. Limestone filler which primarily content calcite, acts as anti-stripping agent to form ionic bond in the surface of granite aggregate and resist moisture damage [27, 57]. Beyond this proportion, the moisture resistance potential declines, reaching a level similar to that of the neat binder. The observed improvement with controlled content of RVO can be attributed to interfacial bonding and the dense structure of the nanomarl. Basically, RVO, being a hydrophobic material, enhances the adhesion between the hydrophobic bitumen and aggregates. This is facilitated by the migration of waste cooking oil to the aggregate surfaces, forming a thin layer that leads to strong interfacial bonds with the bitumen matrix and enhancing its adhesion. This interfacial bonding aids in preventing water ingress and improves the overall moisture resistance of the blend [58, 59]. Additionally, the presence of nanomarl in the blend contributes to the formation of a nanostructured network within the binder matrix. This network enhances the mechanical strength and reduces the permeability of the blend, resulting in improved resistance to moisture.

Rutting potential

Rutting is a common issue observed in asphalt mixtures that have been modified with waste cooking oil, particularly under high temperature conditions and increased traffic loads. Figures 13 and 14 present the rut depth at different cycles for each binder, with the average rut depth also shown in Fig. 14. It can be observed from Fig. 13 that the blend containing 1% RVO and 5%

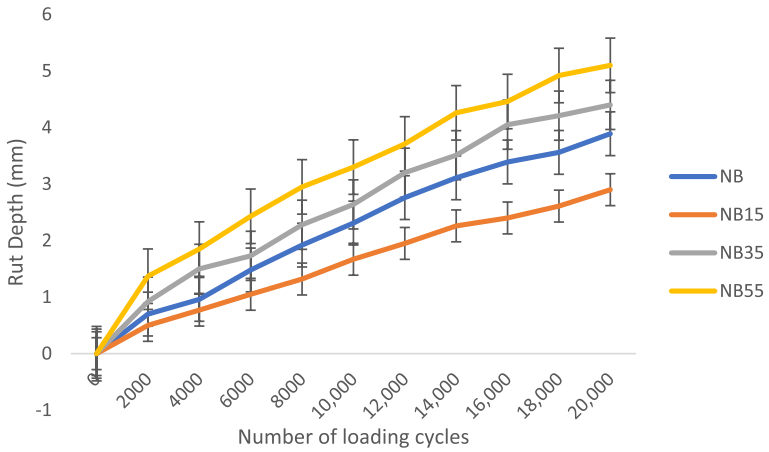

Fig. 13 Rut depth of binders at various cycles

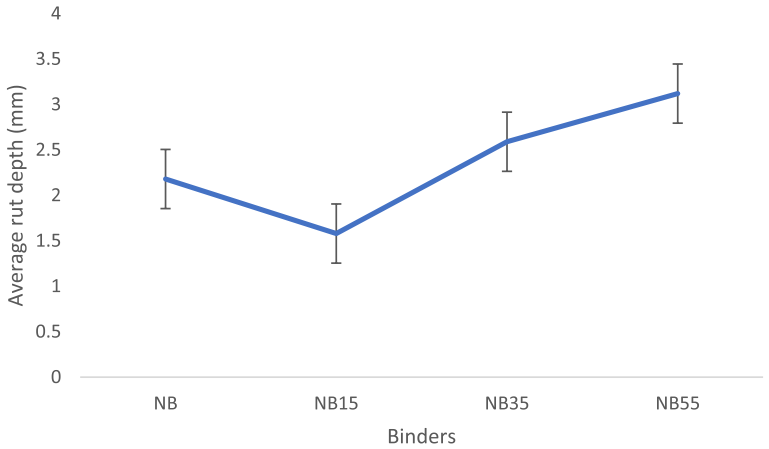

Fig. 14 Average rut depth of binders

nanomarl displayed the smallest rut depth of 2.9 mm after 20,000-wheel load passes. This indicates a significant improvement in rutting potential, with a 13.7% enhancement compared to the neat binder. Similarly, in alignment with the findings from the moisture susceptibility analysis, as the content of RVO increases, the rut depth also increases, reaching its highest value of 4.1 mm when 5% RVO was added. Nanomarl particles introduce a nanoscale reinforcement to the binder, creating a more robust structure. This reinforcement effect, stemming from the extensive surface area and surface morphology revealed in SEM analysis, impedes the movement of binder molecules under stress, thereby contributing to an augmented resistance to rutting. These inherent attributes foster heightened adhesion between the modified binders and coarse aggregates, consequently enhance the resistance to deformation under loading [53].

Microstructure

SEM micrograph

To assess the dispersion characteristics of nanomarl particles within the bitumen-RVO matrix, it is necessary to examine the microstructures of the blend. The SEM micrographs of the neat and modified binders are presented in Fig. 15 (a-b). In Fig. 15 (a), the surface of the neat binder exhibits a continuous dark appearance, indicating a homogeneous bitumen-rich matrix. However, with the addition of up to 5% RVO and nanomarl, as depicted in Fig. 15 (b), fine bright spots become visible on the surface, indicating the homogenous dispersion of nanomarl particles within the blend. The presence of nanomarl particles can alter the surface tension of the modified binder. This change in surface tension affects the wetting behavior of the binder on a surface. As a result, areas with nanomarl particles may have different optical properties, leading

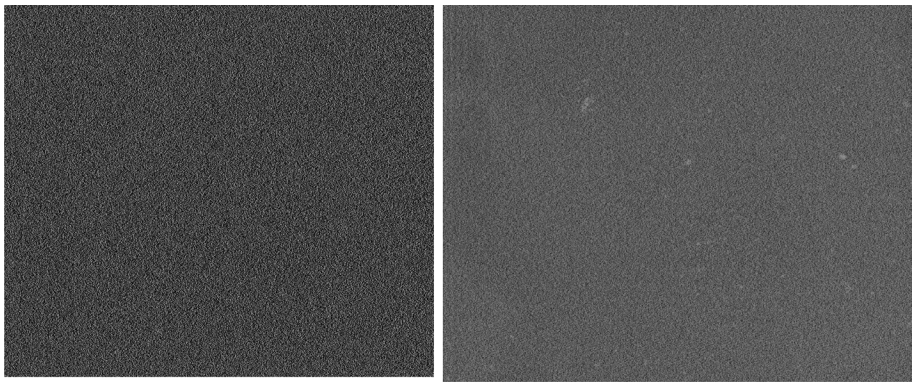

(a) Neat binder (b) Modified binder

Fig. 15 SEM micrograph **a** neat binder **b** modified binder

to the observed bright spots. The fine bright spots on the modified binder's surface indicate the presence of nanomarl particles that are dispersed within the blend. This suggests that there is no phase separation and the nanomarl particles are uniformly distributed throughout the binder matrix.

FTIR analysis

The results of the neat binder and RVO/nanomarl-modified binders are depicted in Fig. 16. In Fig. 16, the presence of characteristic peaks in the range of 2800–3000 cm^{-1} and 1700 cm^{-1} indicates the hydrocarbon stretching and the presence of carbonyl groups, which are associated with the asphaltene and resin fractions in the neat binder. The intensity of the peak around 1740 cm^{-1} and the peak range of 3200–3500 cm^{-1}, attributed to C = O stretching and O–H stretching, respectively, indicate the presence of fatty acid esters in the RVO at the controlled content. Additionally, the characteristic peaks observed in the range of 1000–1100 cm^{-1} are related to the clay structure, specifically the Si–O stretching.

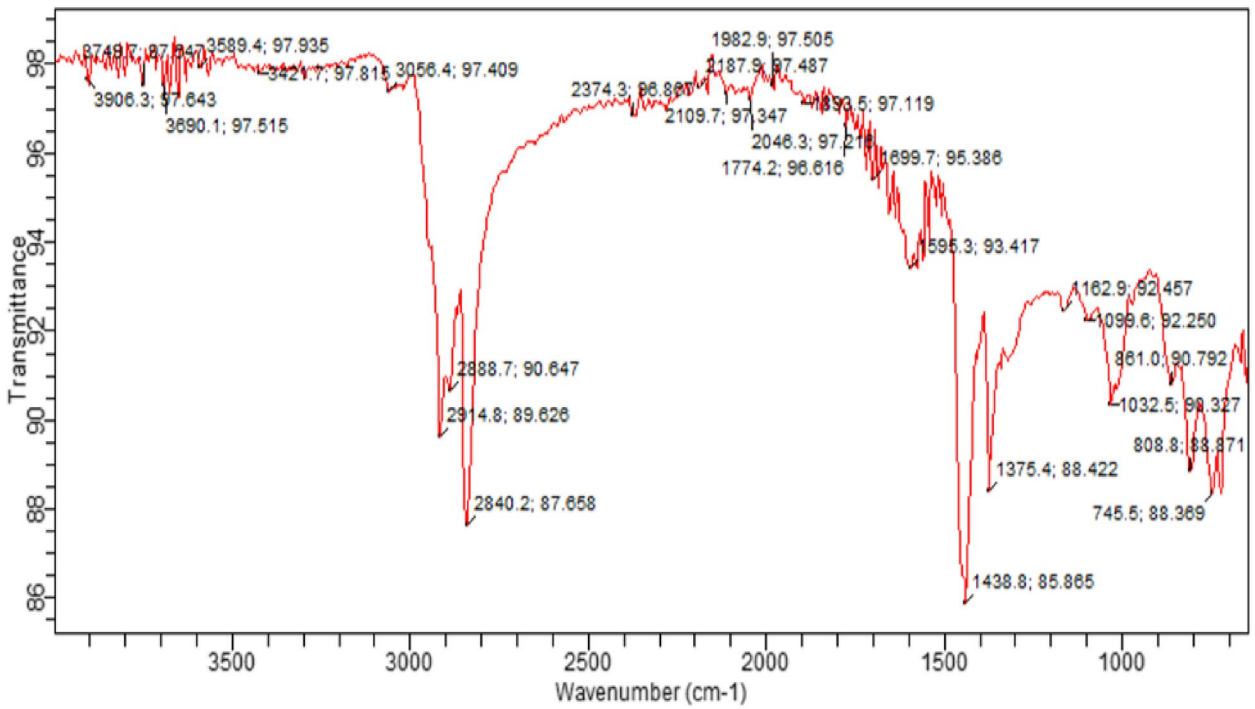

Fig. 16 FTIR Spectrum Analysis for RVO-nanomarl modified bitumen

Table 7 Mixture characteristics

Mixture type	Additive %	OBC (%)	Unit Weight Ton/m^3
Unmodified	0	5	2.320
Modified (RVO and nanomarl)	1 and 5	5	2.326

Cost analysis

Table 7 presents mixture characteristics such as optimum additive percentage, OBC, and the unit weight of modified and unmodified mixtures. Also, Table 8 shows the details about the constituent materials and their associated cost for both modified and unmodified mixtures. Similarly, Table 9 presents the analysis of calculated direct costs for the production of 1 ton of both mixtures. As evidenced by the data in Table 9, the direct cost for producing 1 ton of unmodified mixture stands at N92,508,948, whereas the corresponding cost for 1 ton of the modified mixture is N88,462.335. A comparative analysis of these direct material costs demonstrates the cost-effectiveness of the modified mixtures. The tangible outcome of this financial assessment is a noteworthy savings of approximately N4,046, translating to a substantial cost reduction of 4.57%.

Conclusion

The addition of waste oil can enhance the low temperature performance of the binder and asphalt mixture, but it may have a negative impact on the high temperature performance. However, by incorporating nanomarl into this blend, further improvements can be achieved in the performance of the mixtures, allowing them to withstand temperature variations and traffic loading more effectively. Based on the laboratory experiments conducted and the subsequent analysis performed in this study, the following conclusions can be drawn:

i) The incorporation of RVO in bitumen leads to a gradual increase in the penetration value of the modified bitumen. Simultaneously, the softening point and viscosity of the modified bitumen decrease, suggesting that the addition of oil renders the modified bitumen softer in nature.

Table 8 Materials Cost

Material	Unit	Cost (N)
Bitumen	Ton	620,000
Coarse aggregate	Ton	15,300
Fine aggregate	Ton	5,300
Filler limestone	Ton	9,253
Nanomarl	Ton	8,266
RVO	Ton	3,000

Table 9 Cost analysis

Asphalt Mixture	Unmodified	Modified
Mix unit weight (ton/m^3)	2.320	2.326
OBC (%)	5	5
Weight of bitumen (ton)	0.1160	0.1163
Weight of coarse aggregate (ton)	0.8816	0.8830
Weight of fine aggregate (ton)	1.208	1.1211
Weight of limestone filler (ton)	0.115	0.115
Weight of nanomarl and RVO additives (ton)	-	0.006978
Cost of 1 ton (N)	92,508,948	88,462.335

ii) The inclusion of nanomarl in RVO-modified bitumen enhances its viscoelastic behavior and brings about positive changes in its rheological properties, both in unaged and aged conditions. Specifically, the incorporation of 5% nanomarl results in reduced penetration value, increased softening point, viscosity, rutting resistance, fatigue resistance, creep stiffness, and improved relaxation behavior at low temperatures.

iii) The combination of 1% RVO with 5% nanomarl demonstrated the most favorable outcomes in enhancing both the properties of the binder and the performance of the asphalt mixture.

iv) The microstructural analysis of the blend reveals that the incorporation of additives into the bitumen resulted in successful blending, with no evidence of phase separation. This suggests a homogeneous distribution of the additives within the bitumen matrix.

Appendix

The cost of 1 ton of modified and unmodified asphalt mixtures.

Unmodified asphalt mixture

Optimum bitumen content (OBC) = 5%

Unit weight = 2.320ton/m.^{3}

Weight of bitumen = $\frac{2.320\times5}{100} = 0.116\,tons$

Bitumen cost = weight of bitumen x cost of 1 kg of bitumen.

= 0.116 × N680,000 = N71,920.

Total weight of aggregate = weight of mix – weight of bitumen.

= 2.320 – 0.116 = 2.204 tons.

Coarse aggregate = 40%

Fine aggregate = 54.8%

Filler = 5.2%

Weight of coarse aggregate = $\frac{40}{100} \times 2.204 = 0.8816\,tons$

Coarse aggregate cost = 0.8816 × N15,300 = N13,488.48.
Weight of fine = $\frac{54.8}{100} \times 2.204 = 1.208\ tons$
Fine cost = 1.208 × N5,000 = N6,040.
Weight of filler = $\frac{5.2}{100} \times 2.204 = 0.115\ tons$
Filler cost = 0.115 × N9,253 = N1,060.47.
Total cost of unmodified = N71,920 + N13,488.48 + N6,040 + N1,060.47.
= N92,508.948/tons.

Modified

OBC = 5%
RVO = 1% of 5% weight of mix.
Nanomarl = 5% of 5% weight of mix.
Hence:
Unit weight of mix = 2.326 ton/m.^{3}
Weight of modified binder = $\frac{2.326 \times 5}{100} = 0.1163\ tons$
Weight of RVO = 1% of 0.1163 tons = 1.163×10^{-3} tons.
Weight of nanomarl = 5% of 0.1163 ton = 5.815×10^{-3} tons.
Weight of Neat binder = $0.1163 - 1.163 \times 10^{-3} - 5.815 \times 10^{-3}$
= 0.109322 tons.
Neat binder cost = 0.109322 × N620,000 = N67,779.64.
RVO cost = $1.163 \times 10^{-3} \times$ N3,000 = N3.489.
Nanomarl cost = $5.81 \times 10^{-3} \times$ N8,266 = N48.07.
Total cost of modified bitumen = N67,779.64 + N48.07 + N3.489.
= N67,831.195.
Total weight of aggregate = weight of mix − weight of bitumen.
Weight of coarse aggregate = $\frac{40}{100} \times 2.2097 = 0.8838\ tons$
Coarse aggregate cost = 0.8838 × N15,300 = N13,522.14.
Weight of Fine = $\frac{54.8}{100} \times 2.2097 = 1.2109\ tons$
Fine aggregate cost = 1.2109 × N5,000 = N6,045.
Weight of Filler = $\frac{5.2}{100} \times 2.2097 = 0.115\ tons$
Filler cost = 0.115 × N9,253 = N1,064.
Total cost of modified asphalt = N67,831.195 + N13,522.14 + N6,045 + N1,064.
= N88,462.335/ton.

Acknowledgements
The authors acknowledge support from Cafmeg Laboratory, Shelter Afrique, Nigeria through the use of their laboratory in conducting this research.

Authors' contributions
All authors contributed immensely to the study in the aspect of conceptualization, methodology, laboratory investigations and manuscript writing. Formal analysis of laboratory outcome was jointly carried out by all the authors [Idorenyin Ndarake Usanga], [Fidelis Onyebuchi Okafor], [Chijioke Christopher Ikeagwuani]. Conceptualization of the work, laboratory investigations, results analysis and writing of the first draft of the manuscript was performed by Idorenyin Ndarake Usanga. Laboratory investigation, data analysis and substantial technical contribution in reviewing and editing the work was performed by Chijioke Christopher Ikeagwuani. Laboratory investigation, data analysis and vetting of the draft manuscript was performed by Fidelis Onyebuchi Okafor. All authors read and approved the final manuscript.

Funding
This research did not receive any specific grant from funding agencies in the public, commercial, or not-for-profit sectors.

Availability of data and materials
All data generated and analyze during the study are included in the published article.

Declarations

Competing interests
The authors declare no competing interests.

Author details
[1]Department of Civil Engineering, Akwa Ibom State University, Ikot Akpaden, Nigeria. [2]Department of Civil Engineering, University of Nigeria, Nsukka, Enugu State, Nigeria.

Received: 12 July 2023 Revised: 15 September 2023 Accepted: 19 September 2023
Published online: 24 October 2023

References

1. Behnood A (2019) Application of rejuvenators to improve the rheological and mechanical properties of asphalt binders and mixturea: a review. J Clean Prod 231:171–182
2. Zhang R, Wang H, Gao J, Yang X , You Z (2017) Comprehensive performance evaluation and cost analysis of SBS-modified Bioasphalt binders and mixtures. J Mater Civil Eng https://doi.org/10.1061/(ASCE)MT.1943-5533.0002098
3. Zhang R, You Z, Ji J, Shi Q, Suo Z (2021) A review of characteristics of bio-oils and their utilization as additives of asphalts. Molecules. 2021. https://doi.org/10.3390/molecules26165049
4. Marlene L, Silvia M, Isabel B (2020) Microbial volorization of waste cooking oils for valueable compounds production-a review. Crit Rev Environm Sci Technol 50(24):2583–2616
5. McNally T (2011) Introduction to polymer modified bitumen (PmB). Polymer Modfied bitumen properties and characterisation, 1st ed. Woodhead Publishing, Sawston
6. Bilema M, Aman M, Hassan N. A. (2019) Investigation on rheology and physical properties of asphalt binder blended with waste cooking oil. In: IOP Conference Series: Materials Science and Engineering. IOP Conference Series: Materials Science and Engineering, Kuala Lumpur https://doi.org/10.1088/1757-899X/527/1/012045
7. Ahmad K, Mohd E, Norhidayah H, N. U, Mohd H (2017) Effect of bio based rejuvenator on mix design, energy. In: IOP Conference Series: Earth and Environmental Science. IOP Conference Series: Earth and Environmental Science, Langkawi
8. Guarin A, Abdullah K, Ali B, Björn B, Nicole K (2016) An Extensive Laboratory Investigation of the Use of Bio-Oil Modified Bitumen in Road Construction. Constr Build Mater 106:133–139
9. Wen H, Bhusal S, Wen B (2013) Laboratory evaluation of waste cooking oil based bioasphalt as an alternative binder for hot mix asphalt. ASCE 25(10):1432–1437
10. Kumar S, Negi S (2015) Transformation of waste cooking oil into C-18 fatty acids using a novel lipase produced by Penicillium chrysogenum through solid state fermentation. 3 Biotech 5(5):847–851
11. Ghabchi R, Rani S, Zaman M, Ali S (2019) Effect of WMA additive on properties of PPA-modified asphalt binders containing anti-stripping agent. Int J Pavement Eng 22:1–14
12. Swamy A, Rongali U, Jain P (2017) Effect of HDPEH polymer on viscoelastic properties of SBS modified asphalt. Constr Build Mater 136:230–236
13. Apeagyei A (2011) Laboratory evluation of antioxidants for asphalt binders. Constr Build Mater 53(25):47
14. Ahamad M, Khedmati M, Hahshenas Fatmehsari H (2023) Using crude vegetable-based oils and antioxidants to improve the performance of Asphalt binders. Transp Res Rechttps://doi.org/10.1177/03611981231161607

15. Muhammad Z, Sabzoi N, Srinivasan M, Filippo G (2021) Sustainable asphalt rejuvenation using waste cooking oil: a comprehensive review. J Clean Prod 278(0959–6526):123–304
16. Usanga I, Ikeagwuani C, Etim R, Attah I (2023) Predictive modelling of modified Asphalt mixture rutting potentials: machine learning approach. Iran J Sci Technol Trans Civ Eng https://doi.org/10.1007/s40996-023-01192-w
17. Jiqing Z, Bjorn B, Niki K (2014) Polymer modification of bitumen: Advances and challenges. Eur Polymer J 54:18–38
18. Abdullah M, Zamhari A (2015) A review on the exploration of nanomaterials application in pavement engineering. Jurnal Teknologi 73(4):69–76
19. Xiao F, Amirkhanian A, Amirkhanian S (2011) Influence of carbon nanoparticles on the rheological characteristics of short- term aged asphalt binders. J Mater Civ Eng 23(4):423–431
20. Jahromi S, Andalibizade B, Vossough S (2009) Engineering properties of nanoclay modified asphalt concrete mixtures. Arab J Sci Eng 35(1):89–103
21. Goh S, Michelle A, Zhanping Y, Xianming S (2011) Effect of deicing solutions on the tensile strength of micro- or nano-modified asphalt mixture. Constr Build Mater 25(1):195–200
22. Nazzal MD, Kaya S, Gunay T, Ahmedzade P (2012) Fundamental Characterization of Asphalt Clay Nanocomposites. J Nanomech Micromech 3(1):1–8
23. Danner T, Ostnor T, Justness H (2013) Thermally Activated Marl as a Pozzolan for Cementitious Based Products. In: Twin Covilha International Conference on Civil Engineering-Towards a better environment and The Concrete Future. Conference: Twin Covilha International Conference on Civil Engineering, Covilha
24. Vakili A, Narimousa R, Salimi M, Farhadi M, Dezh M (2019) Effect of free flaw cycles on characteristics of Marl Soils treated by electroosmosis applications. Cold Reg Sci Technol https://doi.org/10.1016/j.coldregions.2019.10.2861
25. Nailia R, Ravil R, Vladimir M, Albert G, Ludmila P, Alfiya G, Yury O (2018) Marl-based geopolymers incorporated with limestone: A feasibility study. J Non-Cryst Solids 492:1–10
26. Bahhou A, Yassine T, Elkhessaimi Y, Hakkou R, Tagnit-Hamou A, Benzaazoua M (2021) Using Calcined Marls as Non-Common Supplementary Cementititious Materials. Minerals 11(3):517–539
27. Usanga I, Okafor F, Ikeagwuani C (2023) Investigation of the performance of hot mix Asphalt enhanced with calcined marl dust used as fillers. Int J Pavement Res Technol https://doi.org/10.1007/s42947-023-00323-w
28. ASTM D5, American Society for Testing and Materials (2006) Standard test methods for penetration of bituminous materials. ASTM, Pennsylvania
29. ASTM D36, American Society for Testing and Materials (2006) Standard test methods for softening point of bitumen (Fing and ball apparatus). ASTM, Pennsylvania
30. ASTM D4402, American society for testing and materials (2022) Standard test method for viscosity determination of asphalt at elevated temperatures using rotational viscometer. ASTM, Pennsylvania
31. ASTM D 92, American society for testing and materials (2020) Standard test method for determination of flash point using a Prensky-martens closed-up apparatus. ASTM, Pennsylvania
32. ASTM D 70, American society for testing and materials (2003) Standard test method for density of semi solid bituminous materials (Pycnometer method). ASTM, Pennsylvania
33. ASTM D 5821, American society for testing and materials (2017) Standard test method for determing the percentage of fractured particles in coarse aggregate. ASTM, Pennsylvania
34. ASTM D 4791 American society for testing and materials (2010) Standard test method for flat particles, elongated particles. ASTM, Pennsylvania
35. ASTM C88, American society for testing and materials (2018) Standard test method for soundness of aggregates. ASTM, Pennsylvania
36. ASTM C127, American society for testing and materials (2016) Standard test method for relative density and absorption of coarse aggregate. ASTM, Pennsylvania
37. ASTM C131, American society for testing and materials (2010) Standard test method for resistance to degradation of small-size coarse aggregate by abrasion and impact in the Los Angeles machine. ASTM, Pennsylvania
38. ASTM C128, American society for testing and materials (2016) Standard test method for density, relative density and absorption of fine aggregate. ASTM, Pennsylvania
39. ASTM D2419, American society for testing and materials (2022) Standard test method for equivalent value soil and fine aggregates. ASTM, Pennsylvania
40. ASTM C142, American society for testing and materials (2017) Standard test method for clay lumps and friable particles. ASTM, Pennsylvania
41. ASTM C854, American society for testing and materials (2002) Standard test methods for specific gravity of soil solids by water pycnometer. ASTM, Pennsylvania
42. ASTM C204, American society for testing and materials (2004) Standard test method for fineness of hydraulic cement by air permeability apparartus. ASTM, Pennsylvania
43. ASTM D546, American society for testing and materials (2017) Standard test method for sieve analysis of mineral filler for asphalt paving mixtures. ASTM, Pennyslvania
44. Langa E, Buonocore G, Squillace A, Muiambo H (2023) Effect of vegetable oil on the properties of asphalt binder modified with high density polyethylene. Polymers 15(3) https://doi.org/10.3390/polym15030749
45. ASTM D1559, American society for testing and materials (200) Standard test method for Marshall test. ASTM, Pennsylvania
46. AASHTO T 315 (2010) Determining the rheological properties of asphalt binder using a Dynamic Shear Rheometer (DSR). AASHTO, Washington, D.C.
47. AASHTO T 240 (2022) Standard method of test for effect of heat and air on a moving film of asphalt binder (Rolling Thin-Film Oven Test). AASHTO, Washington, D.C
48. A. T1313 (2022) Standard method of test for determining the flexural creep stiffness of asphalt binder using the Bending Beam Rheometer (BBR). AASHTO, Washington, D.C
49. AASHTO T 283. American association of state highway and transportation officials (2022) Standard method of test for resistance of compacted asphalt mixtures to moisture-induced damage. AASHTO, Washington, D.C
50. AASHTO T 324 (2014) Hamburg wheel-track testing of compacted hot mix Asphalt (HMA). AASHTO, Wasgington, D.C
51. Li R, Xiao F, Amirkhanian S, You Z, Huang J (2017) Developments of nano materials and technologies on asphalt materials-A review. Constr Build Mater 143:633–648
52. Bala N, Kamaruddin I, Napiah M, Nahi M (2017) Influence of nanosilica on rheological properties and oxidative aging of polymer modified bitumen. J Eng Appl Sci 12(22):5990-5996
53. Golestani B, Nam B, Nejad F, Fallah S (2015) Nanoclay application to asphalt concrete: Characterization of polymer and linear nanocomposite-modified asphalt binder and mixture. Constr Build Mater 91:32–38
54. Fang C, Yu R, Li Y, Zhang M, Hu J, Zhang M (2013) Preparation and characterisation of an asphalt-modifying agent with waste packaging polyethylene and organic montmorillonite. Polym Test 32(5):953–960
55. Lowry E, Piri M (2018) Effect of surface chemistry on confined phase behavior in Nanoporous media: an experimental and molecular modeling study. Langmuir 34(32):9349–9358
56. AASHTO M320 (2010) Standard specification for performance-graded asphalt binder. AASHTO, Washington, D.C
57. Soenen H, Vansteenkiste S, Demacijer P (2020) Fundamental approaches to predict moisture damage in asphalt mixtures: state -of -the -art review. Infrastructures 5(2). https://doi.org/10.3390/infrastructures5020020
58. Bagampadde U, Isacsson U, Kiggundu B (2004) Classical and contemporary aspects of stripping in bituminous mixes. Road Mater Pavement Design 5:7-43. https://doi.org/10.1080/14680629.2004.9689961
59. Iwanski M (2020) Effect of hydrated lime on indirect tensile stiffness modulus of asphalt concrete produced in half- warm mix tehnology. Materials 13:4731. https://doi.org/10.3390/ma13214731

Publisher's Note